eprints@whiterose.ac.uk
https://eprints.whiterose.ac.uk/

Bubble-based EMMS mixture model applied to turbulent fluidization

Atta Ullah[a,*], Kun Hong [b], Wei Wang[c], Stephen Chilton[d], William Nimmo[e]

[a]Department of Chemical Engineering, Pakistan Institute of Engineering and Applied Sciences, 45650, Pakistan

[b]College of Life Science and Chemical Engineering, Huaiyin Institute of Technology, Huaian, 223003, China

[c]Institute of Process Engineering, Chinese Academy of Sciences, Beijing, 100190, China

[d]Energy Research Institute, University of Leeds, Leeds LS2 9JT, UK

[e]Dept of Mechanical Engineering, The University of Sheffield, Sheffield, S10 2TN

[*] Corresponding author. Tel.: +92 (51) 1111 74327; E-mail address: atta@pieas.edu.pk

Abstract

Turbulent fluidization is now widely recognized as a distinct flow regime and is commonly utilized in industrial fluidized-bed reactors. However, relatively fewer attempts have been made to rigorously model these systems in comparison to bubbling and circulating fluidized beds. In this work, we have rewritten the original bubble based EMMS model in form of a mixture to apply it to turbulent fluidization. At microscale this mixture is composed of gas and particles whereas voids and gas-particle suspension make up this mixture at mesoscale level. Subsequently, all the system properties are then calculated in terms of mixture rather than individual phases. With the minimization of the objective function for the bubbling mixture, the set of equations is then solved numerically. The objective function, used to close the system of equations, is composed of the energy consumption rates required to suspend gas-particle suspension and the energy consumed due to interaction between suspension and voids. The model is then applied to simulate gas-solid turbulent fluidized beds. Simulation results are encouraging as the model is able to predict the dense bottom and dilute top zones along the height of the bed. Comparison of results with experimental data and homogeneous drag model has been made for validation purposes.

Keywords: Turbulent fluidization; Mesoscale; Bubble; EMMS; Mixture; CFD; Modeling

1. Introduction

Gas-solid flows display heterogeneity over a wide range of spatial and temporal scales covering regimes from bubbling to pneumatic transport. Matheson et. al. [1] were the first ones to show photographs of turbulent fluidization, which were significantly different from bubbling fluidization [2]. However, turbulent fluidization has only been widely recognized as a distinct flow regime for the past couple of decades, occurring between the bubbling and the high velocity fluidization regimes [3]. Extensive details about the identification and characterization of the turbulent fluidization regime can be found in published literature such as the work by Martin Rhodes [4] and John Grace [5].

Turbulent fluidization is widely used due to its vigorous gas–solids mixing, favorable bed-to-surface heat transfer, high solids hold-ups (typically 25–35% by volume), and limited axial mixing of gas [2]. It is considered to be a transition from the bubbling to the transport regime which occurs due to a change in the mechanism of bubble formation and breakage. Moving from bubbling to turbulent fluidization, the hydrodynamics of the bed change from a regime of bubble

formation and coalescence dominant mechanism to a regime with breaking and gradual disappearance of the large bubbles [6]. In turbulent beds, a sigmoidal profile for the solids hold-up is generally observed. Therefore, turbulent fluidized bed is characterized by two different coexisting regions: a lower region where solids are the continuous phase and gas the dispersed phase and an upper region, where gas is the continuous phase and solids are dispersed [7].

Two major approaches have been followed in attempts to apply CFD modeling to gas-solid fluidized beds: Eulerian two-fluid models and Euler/Lagrangian models [8]. Euler/Lagrangian method is generally limited due to the number of solid particles it can handle. Therefore, the Eulerian modeling has become a preferred choice for simulation of large macroscopic systems. In this approach, the gas and solid phases are assumed to be fully interpenetrating continua [9]. This methodology has been adopted widely by several investigators to model turbulent fluidized beds [10-14]. This approach requires either fine-grid resolution of the flows or modification of simulation parameters to incorporate sub-grid structures [15-19]. Although there has been some progress towards accurate resolution of the sub-grid scale structures but to date no unified approach exists. In fact, some studies have reported that the Eulerian two-fluid models with the homogeneous drag model fails to capturing typical features of gas-solid flows even with high resolutions [14, 20]. Under such circumstances, the Eulerian two-fluid model may not be able to correctly reflect the effects of these sub-grid structures. Thus it may be difficult to reproduce the multi-scale nature of such heterogeneous flows unless their effects are considered in the constitutive closure laws governing these flows.

To consider the effects of these mesoscale structures, a practical approach is to modify the homogeneous correlation based drag coefficients and stresses etc. with structure-based entities in addition to the resolved parts of two-fluid simulations. In this context, in recent years there has been significant improvement. Some authors [21-23] have used empirical correlations or equivalent cluster diameters to modify the homogeneous drag force. Others have considered heterogeneity by modifying the drag coefficient through the cluster-based EMMS (energy-minimization multi-scale) approach [24-26]. Recently there has been attempt to model the bubbling bed heterogeneity by following the EMMS principle [27]. This bubble-based EMMS model has also been applied to simulate riser flow [28]. Although progress has been made, but a unified model is still far from available.

While many efforts have been dedicated to model and simulate bubbling and transport type systems such as risers of CFBs, turbulent fluidization has received relatively less attention in terms of modeling and simulation. An attempt by using the four zoned drag model approach to simulate turbulent fluidized bed has been made recently [11, 29]. Adopting a similar multi-zoned drag model, Gao et al. [13] simulated their turbulent fluidized bed in fair agreement with their experimental data. In another recent attempt, Hong et al. [30] extended the work of bubble based EMMS model of Shi et al. [27] by coupling the structure-dependent multi-fluid model (SFM) to model heterogeneous gas-solid flows including turbulent fluidization. These attempts reflect the interest of modellers in correct prediction of hydrodynamics of turbulent fluidized beds where the outlet solids flux is negligible.

The theme of current work is the fact that the drag force and stresses in uniform gas-solid systems are significantly different from the real systems due to the existence of heterogeneous structures. These structures can be in the form of bubbles and/or clusters, depending upon the operating conditions. In this current work on turbulent fluidized bed modeling, we have followed

this structure dependent drag model approach by considering the system to be in the form of a mixture at both micro and mesoscale level. This model may be considered as an alternate representation of earlier work of Shi et al. [27] from our group. Details of the model formulations are presented in the next section. Then some discussion about the model results is made. Finally the modified drag from mixture formulation is used to simulate turbulent fluidized bed and the results are validated against available experimental data.

2. Mathematical formulation of bubble-based EMMS mixture model

In the terminology of structure dependent multi-fluid model of Hong et al. [18], the system can be decomposed into four components i.e. dilute-phase gas, dilute-phase solid, dense-phase gas and dense-phase solid. Here we consider two mixtures existing simultaneously i.e. "gas & particles" at microscale known as the "dense phase" and "dense phase & void phase" at mesoscale where the void phase is assumed to be free of particles.

Following the same approach as previously for the development of EMMS models, a complete set of balance equations can be written at micro, meso and macro scales. For simplicity, we have summarized all the relevant definitions and parameters in appendix Table A.1. In the development of this model, only the vertical scalar components have been used. As a first approximation, inertial and interphase exchange terms were neglected and the bubbles/voids are considered to be completely free of solid particles. After obtaining the final form of drag force correlations, all the inertial effects were lumped into a single acceleration term. Furthermore, there is no net solids flux out of the column. Effectively, there are two dominant forces at play i.e. drag due to gas in particles inside dense phase and drag due to existence of mesoscale bubbles in the dense emulsion phase. Following set of equations can be written for such a system.

o Gas mass balance: mass flow rate of the gas phase across any cross-section of the bed is equal to the sum of the gas flow rate through dense and dilute phases individually.

$$U_g = fU_{gc} + (1\text{-}f)U_{gf} \quad (1)$$

o Mean bed voidage: the mean voidage of the bed can be obtained from the dense and dilute phases as

$$\varepsilon_g = f\varepsilon_{gc} + (1\text{-}f)\varepsilon_{gf} \quad (2)$$

Where the voidage of dilute phase, ε_{gf}, has been assumed 1 in current formulation.

o Force balance for solid particle in the dense phase: Using equations for individual phases presented in Wang and Li [25] and following the approach for mixture modelling [31], we have the drag force for dense phase as

$$m_c F_c = \frac{f(1-\varepsilon_{gc})}{\pi d_p^{3}/6} C_{d_0,c}\varepsilon_{gc}^{-2.7}\left(\frac{\rho_f}{2}\right)\left(\frac{\pi d_p^{2}}{4}\right)U_{slip,c}^{2} = \frac{f(\rho_{mc}-\rho_{mi})(a_m-g)}{(1-f)} \quad (3)$$

o Force balance for mesoscale bubbles in unit control volume: the drag force of the emulsion-like dense phase exerted on bubbles is equal to the effective buoyancy of bubbles in unit control volume.

$$\left(m_i F_i\right)_b = \frac{1-f}{\pi d_b^{3}/6} C_{d_0,i} f^{-4.7}\left(\frac{\rho_{mc}}{2}\right)\left(\frac{\pi d_b^{2}}{4}\right)U_{slip,i}^{2} = (1-f)(\rho_{mi}-\rho_f)(a_m-g) \quad (4)$$

Where d_b is the characteristic diameter of the bubble/void calculated from a suitable closure.

o Pressure drop balance between the dense and void phases: the gas flowing in the bubbles/voids will have to support the dense-phase particles. The resultant pressure drop equality yields

$$m_i F_i = (1-f) m_c F_c \quad (5)$$

Thus

$$m_c F_c = \frac{m_i F_i}{(1-f)} = \frac{-f(\rho_{mc} - \rho_{mi})g}{(1-f)} \quad (6)$$

It is now easy to lump all the inertial terms into a single variable and add to the steady system. Thus with respective accelerations, we have

$$m_i F_i = f(\rho_{mc} - \rho_{mi})(a_{mi} - g) \quad (7)$$

$$m_c F_c = \frac{f(\rho_{mc} - \rho_{mi})(a_{mc} - g)}{(1-f)} \quad (8)$$

Furthermore, due to equal pressure drop relation, inertial terms can be simplified as

$$a_{mc} = a_{mi} = a_m \quad (9)$$

The last expression signifies a fact that under the current model setup, both the micro and mesoscales move with same acceleration.

o Bubble diameter: We have followed the correlation of Horio and Nonaka's [32] for the prediction of bubble characteristics of fluidized bed. Hence, the bubble diameter can be calculated with the expressions stated below.

$$d_b = \frac{\left[-\gamma_M + \left(\gamma_M^2 + 4d_{bm}/D_t \right)^{0.5} \right]^2 D_t}{4} \quad (10)$$

Where

$$\gamma_M = \frac{2.56 \times 10^{-2}}{U_{gc}} \sqrt{\frac{D_t}{g}} \quad , \quad d_{bm} = \frac{2.59}{g^{0.2}} \left[\frac{(U_g - U_{gc})\pi D_t^2}{4} \right]^{0.4}$$

o Stability criterion:

$$N_{st,mix}/N_T \rightarrow \mathbf{min} \quad (11)$$

Where $N_{st,mix}$ can be reformulated as,

$$\left(N_{st,mix} \right)_b = \frac{1}{(1-\varepsilon_g)\rho_s} \left[\left(\frac{f(\rho_{mc} - \rho_{mi})}{(1-f)} \right) fU_{fc} + f_b U_f \right] g \quad (12)$$

Where we follow the definition of f_b from Shi et al. [27], which is given as

$$f_b = \frac{1-f}{(1-f)+f\varepsilon_{gc}}$$

and

$$N_T = \frac{(\rho_p - \rho_f)U_f g}{\rho_p}$$

With the given operating conditions (U_g) and the mean bed voidage (ε_g), above stated set of equations along with the stability criterion can be solved to obtain seven structural parameters (d_b, f, ε_{gc}, U_{gf}, U_{gc}, U_{sc}, a_m). The solution scheme is essentially the same as in Wang and Li [25]. Once the system of equations has been solved for any voidage satisfying the stability criterion, the drag coefficient is then calculated as

$$\beta = \frac{\varepsilon_g^{\ 2}}{U_{slip}} F_d = \frac{\varepsilon_g^{\ 2}}{U_{slip}} \left[\frac{f(\rho_{mc} - \rho_{mi})}{1-f} + (1-f)(\rho_{mi} - \rho_g) \right](a_m - g) \quad (13)$$

For comparison, the standard drag coefficient for homogeneous dispersions i.e. Wen-Yu is calculated as in Wang and Li [25]. Then heterogeneity index, H_d, is calculated as

$$H_d = \frac{\beta}{\beta_{WY}} \quad (14)$$

Where β_{WY} is Wen and Yu [33] correlation with

$$\beta_{WY} = \frac{3}{4} C_{d0} \frac{\varepsilon_g \varepsilon_s}{d_p} \rho_g \left| \mathbf{u}_g - \mathbf{u}_s \right| \varepsilon_g^{-2.7} \quad (15)$$

3. CFD simulation of turbulent fluidized bed with the EMMS drag

Two dimensional CFD simulation of the turbulent fluidized bed (TFB) of Venderbosch [6] has already been carried out by using a similar model with Eulerian multiphase flow modeling approach available in ANSYS Fluent®. The results of that study are presented in our recent article in proceedings of CFB-11 [34]. Current study is to extend previous approach, test and validate the model developed here. In what follows, we have used Group-B particles (Geldart's classification) to test the grid independence and find the appropriate boundary conditions for the solid phase. The findings are then used to model a turbulent fluidized bed of Group-A particles. The heterogeneity indexes obtained from the solution of above mentioned EMMS model are shown in Fig. 1 and have been used in the current study. It is to be pointed out here that the particles with lower Archimedes number require major drag correction as compared to those with higher Archimedes number. This trend can also be observed in the work of Hong et al. [18] where three different types of particle systems were simulated. Although the EMMS model used there was based on cluster description of heterogeneous structures. This variation of drag correction based on particle characteristics can be a potential area of research.
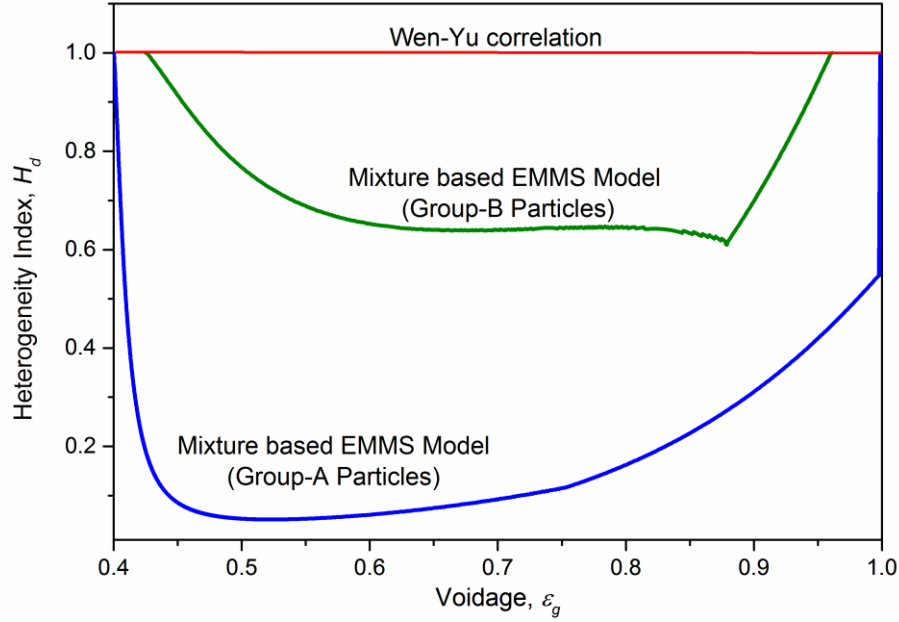
Figure 1 Heterogeneity index H$_d$ as a function of mean voidage for the turbulent fluidized systems used for simulation.

3.1 Governing equations and assumptions

Keeping in view the computational cost required by extensive simulations, the Eulerian two-fluid model (TFM) is a practical approach to simulate large-scale reactors. The present simulations are based on the TFM approach available in ANSYS Fluent 14.5®. Table A.2 in Appendix lists the governing equations that the software solves for the TFM simulation. For current purposes, the heterogeneity index obtained in Eq. (15) is fed to the software as a user-defined function (UDF) to correct the Wen-Yu's homogeneous drag model. Kinetic theory of granular flow (KTGF) developed by Gidaspow [9] has been used to close the properties of solid phase. The structure dependent stresses have been neglected in current study. The hydrodynamics of the system have been assumed to be governed by laminar flow conditions in current work. Furthermore, in this work, the granular energy has been assumed to be at steady state so that it is dissipated locally. This assumption allows us to neglect the convection and diffusion terms in the granular temperature transport equation. This assumption is valid under dense bed conditions such as bubbling and turbulent fluidized beds [35].

3.2 Simulation of turbulent fluidized bed with Group-B particles
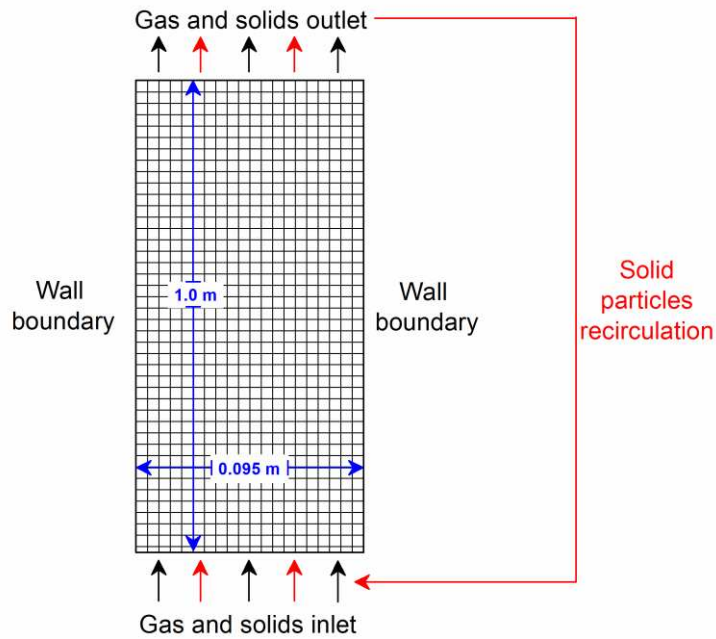
Figure 2 Schematic of the turbulent fluidized bed setup used for simulation.

Fig. 2 represents the layout of the simulation setup with Group-B particles adopted from Gao et al. at Zhejiang University (China) [13]. Initially the bed is packed to a height of 0.204m with solids concentration of 0.55. Inlet superficial air velocity is set to be 1.25m/s. Bed is composed of spherical particles with a diameter of 139μm and a density of 2400kg/m^3. Under these operating conditions, the particles have a minimum fluidization velocity of 0.091 m/s and terminal velocity of 1.2 m/s. Physical properties of the system used for current CFD study are summarized in Table 1. The solids exiting the top of the column are recirculated back to the column with same flux. For grid independence study, the meshes with 20×200, 40×200, 40×250, 40×320 grids were used. For grid independence study, both the gas and solids phases were not allowed to slip at the wall. A time step of 5×10^{-4}s was used. A maximum of 50 iterations were allowed for each time step. The convergence criterion for two successive iterations was set to the default value of 0.001. All simulations were carried out for 30s of physical time. The statistics for time-averaging were collected for a period of last 15s.

The results of grid independence study are presented next. Then a comparison of the model results with homogeneous drag model will be made. Lastly, the effect of boundary conditions on bed profiles will be presented.

Table 1 Modeling parameters for Group-B fluidized system of Gao et al. [13] used in this study

| Parameter	Value
Gas density	1.225kg/m^3
Gas viscosity	1.789x10^{-5}kg/(m.s)
Particle diameter	139μm
Particle density	2400kg/m^3
Bed diameter	0.095m

|	
Bed height	1 m
Initial bed height	0.204m
Inlet gas velocity	1.25m/s
Inlet boundary condition	Velocity inlet
Outlet boundary condition	Atmospheric pressure
Wall boundary condition for gas phase	No slip
Wall boundary condition for solid phase	No slip and partial slip
Maximum packing limit	0.63
Restitution coefficient	0.9
Time step	0.0005s
Convergence criterion	0.001

3.2.1 Grid independence

Fig. 3(a) shows the axial voidage profiles for the four grids used in the current grid independence study. All the grids are able to predict the dense bottom and dilute top region, which shows that the current drag model is capable of predicting correct qualitative trend. A close looks shows that the difference between the two fine grids i.e. 40×250 and 40×320 is not significant. Therefore, for further simulation purposes the grid resolution of 40×250 was chosen which corresponds to 17 particle-diameters laterally and about 28 particle-diameters axially. These results are encouraging as it is generally accepted that for grid-independence of gas-solid flows grid size should be around 10-particle-diameters [36]. Such a fine mesh for large reactors will require much larger computational power. Fig. 3(b) shows instantaneous snapshots of solids concentration in the bed. It can be observed that with the grid refinement, the overall height of the bottom dense region decreases and it becomes denser.
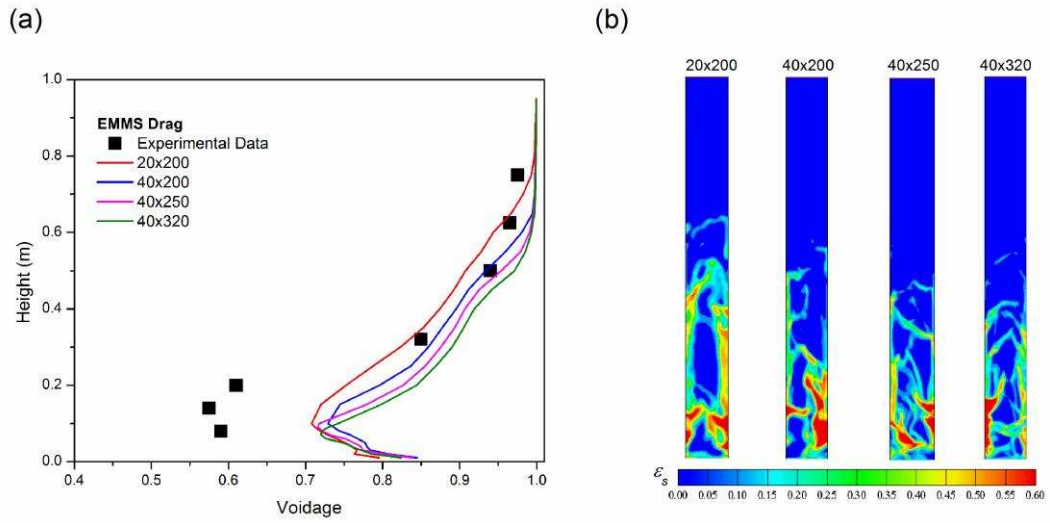
Figure 3 (a) Time-averaged profiles of voidage along the bed height for different grid sizes; (b) Instantaneous solid fraction in the bed.

3.2.2 Comparison of results for the EMMS and homogeneous drag models

Fig. 4 shows the comparison of both the axial and radial profile predictions of the EMMS drag model and the Gidaspow drag model. Looking at the axial voidage profiles in Fig. 4(a), it can be observed that the homogeneous drag model is able to predict a dense bottom zone which smoothly diffuses to low voidage towards the top. However, there is not a sharp transition from the dense bottom to dilute top region. On the other hand, the EMMS model is capable to predicting the dense and dilute regions with sharp transition in between. As compared to the homogeneous model, the solid fraction predicted by EMMS model in the bottom zone is higher. Furthermore, the agreement with the experimental data for EMMS model is also encouraging. In Figs. 4(b) and 4(c), the radial profiles of the solid fraction predicted by the two models are not significantly different, although the predictions of EMMS model are relatively nearer to the experimental data. We speculate that the current EMMS model needs to be tested for different treatment at wall. This is what is presented next.
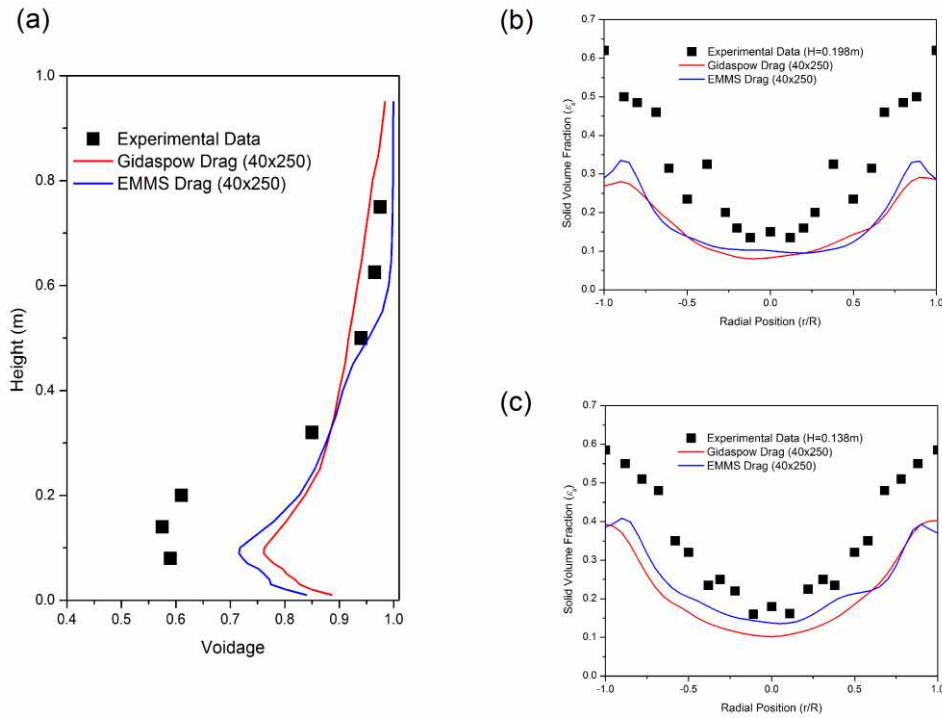
Figure 4 Comparison of results for EMMS drag model with Gidaspow drag model: (a) Time-averaged axial voidage profile; (b) Time-averaged radial solid fraction profiles at a height of 0.198m; (c) Time-averaged radial solid fraction profiles at a height of 0.138m.

3.2.3 Effect of wall boundary condition

In this section, we present a comparison of the axial and radial profiles of the bed voidage/solid fraction. The modified boundary condition was set for partial slip of solid particles at the wall. To achieve this, a specularity coefficient of 0.0001 was specified as recommended in published literature [37]. It can be seen from the results presented in Fig. 5 that this partial slip boundary condition allows for better prediction of the height of bottom dense phase. It is to be expected as with partial slip more solids are allowed to move up the column. Furthermore, the predictions of the EMMS model's radial profiles for both the heights of 0.138m and 0.198m are in very good agreement with the experimental data. The Gidaspow drag model, however, is not able to accurately predict the dilute core-annulus type behavior
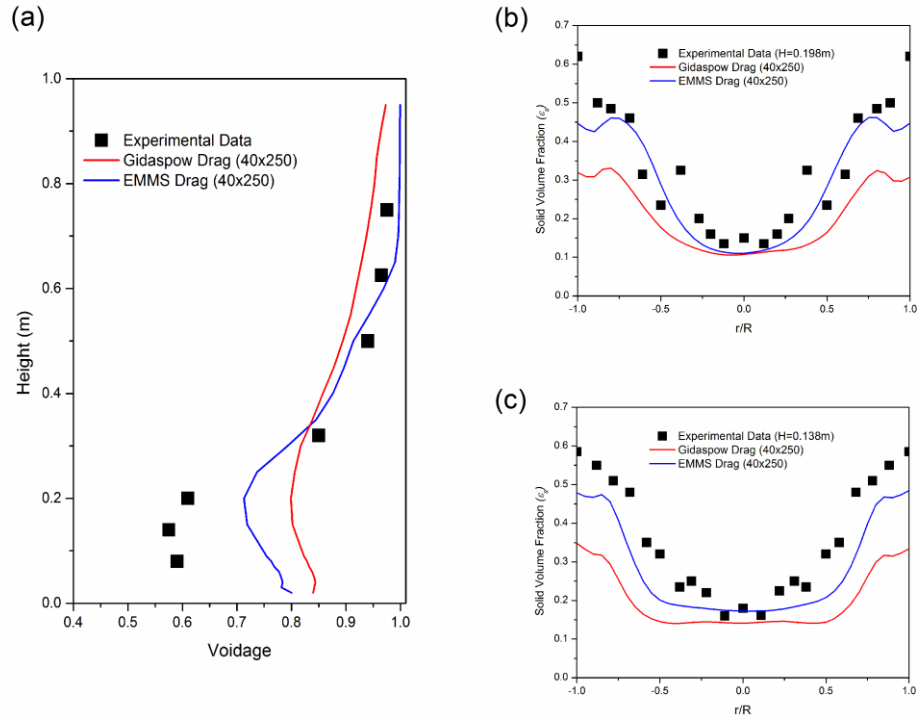
Figure 5 Effect of wall boundary condition on the time-averaged profiles for both EMMS and Gidaspow drag model: (a) Axial voidage profiles; (b) Radial solid fraction profiles at a height of 0.198m; (c) Radial solid fraction profiles at a height of 0.138m.

3.2.4 Conclusions from study of Group-B particles

From the simulation results presented above, it can be deduced that the grid resolution corresponding to about 20-30 particle-diameters may be sufficient for simulation of turbulent fluidized beds with present EMMS model. However, it is recommended to test grid independence before implementing the model for any practical purposes. Furthermore, as observed, the boundary condition accounting for the partial slip of the solid particles at the wall is suitable for prediction of correct radial voidage profiles. Based upon these conclusions, we now attempt to simulate the turbulent fluidized bed with fine particles of Gao et al. [11] at China University of Petroleum (Beijing) in the next section.
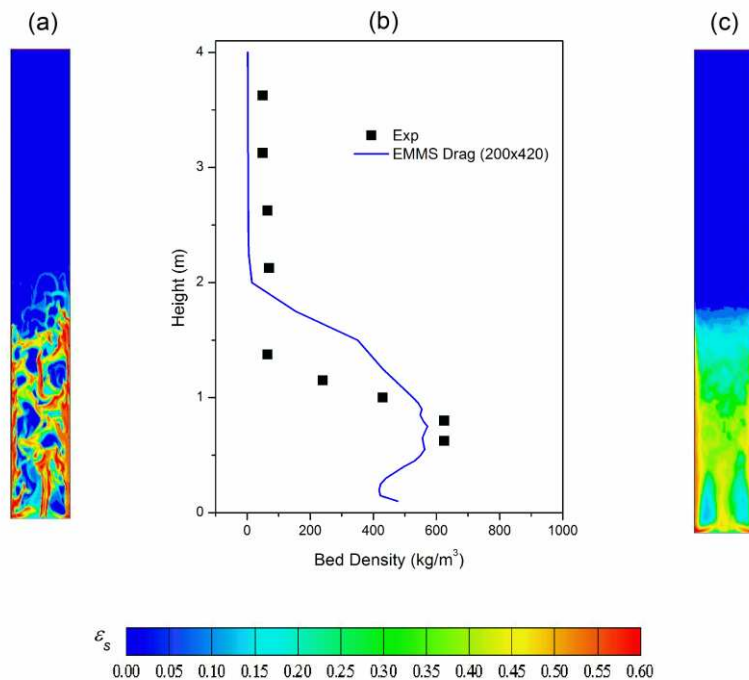
3.3 Simulation of turbulent fluidized bed with Group-A particles

The simulation layout of the setup for the turbulent fluidized bed of Group-A FCC particles is essentially the same as for Group-B particles. The dimensions of the bed have increased now. The bed for this new is now 4m high and has lateral dimension of 0.5m. The conditions now are such that initially the bed is packed with FCC particles to a height of 1 m with a packing fraction of 0.55. The superficial gas velocity at the inlet is set to be 0.5m/s. Particles in the bed are of spherical with a diameter of 60µm and have a density of 1500kg/m^3. The minimum fluidization and terminal velocity for this system is 0.0047m/s and 0.58m/s respectively. The solids leaving at the top of the column are fed back to the column with the same mass flux. We have only simulated one mesh size here such that the bed is divided into 200×420 grid cells. The aim is to test the capabilities of this new EMMS drag model. Based upon the conclusions drawn from previous

section, the gas was not allowed to slip at wall while partial slip with specularity coefficient of 0.0001 was implemented for solid particles. Transient simulation was carried out with a time step of 5×10^{-4}s. A maximum of 50 iterations were allowed for each time step. The convergence criterion for two successive iterations was set to the default value of 0.001. All simulations were carried out for 30s of physical time. The statistical time-averaging data was collected for a period of the last 10s. Summary of simulation parameters is given in Table 2.

Table 2 Modeling parameters for Group-A fluidized system of Gao et al. [11] used for study

Parameter	Value
Gas density	$1.225kg/m^3$
Gas viscosity	$1.789x10^{-5}kg/(m.s)$
Particle diameter	$60\mu m$
Particle density	$2400kg/m^3$
Bed diameter	0.5m
Bed height	4m
Initial bed height	1m
Inlet gas velocity	0.5m/s
Inlet boundary condition	Velocity inlet
Outlet boundary condition	Atmospheric pressure
Wall boundary condition for gas phase	No slip
Wall boundary condition for solid phase	Partial slip (specularity coefficient = 0.0001)
Maximum packing limit	0.63
Restitution coefficient	0.9
Time step	0.0005s
Convergence criterion	0.001

Figure 6 Simulation results of turbulent fluidized bed with Group-A particles using EMMS drag model: (a) Snapshot of instantaneous solid fraction in the bed; (b) Axial voidage profile; (c) Time averaged snapshot of solid fraction in the bed.

The results of Fig. 6 indicate that qualitatively correct bed density profile made up of dense bubbling type bed at the bottom and dilute region at the top, can be reproduced using the present EMMS drag model in conjunction with TFM. However, some fine tuning is needed for accurate prediction of experimental data. Solids entrainment may contribute to such discrepancy though further analysis needs to be carried out in future work. For example, the effect of restitution coefficient was not analyzed in this work. Furthermore, the approximation of algebraic granular temperature model was used in present work. This approximation may not be valid in the top dilute region. It may be beneficial to study the results the using full partial differential equation for granular temperature. Furthermore, the effect of boundary conditions also needs to be assessed for this system with lower Archimedes number. However, these studies are beyond the scope of present work.

4. Conclusion

Following the approach of multiscale modeling, the work presented in this manuscript reports the development of a bubble-based EMMS mixture model. The solution of the model shows that the model can capture the drop in drag coefficient due to the presence of mesoscale bubbles. The application of the model to turbulent fluidization has shown good agreement between the simulated and experimental data. By using the current drag model under the umbrella of TFM framework, it is possible to capture the sigmoidal voidage profile of turbulent fluidized beds. Using the conclusions from current work, it is possible to extend the current mixture model for application to riser type flows where solid carryover becomes an operating parameter. Furthermore, to carry out accurate modeling of dense beds the effects of mesoscale structures on particle stresses also needs to be accounted for. Hence further work needs to be carried out in future.

Nomenclature

Ar	Archimedes number, dimensionless
a	inertial term, m/s^2
C_d	effective drag coefficient for a particle or a bubble
C_{d0}	standard drag coefficient for a particle or a bubble
d_b	bubble diameter, m
d_p	particle diameter, m
D_t	column diameter, m
e_s	particle-particle restitution coefficient
e_w	particle-wall restitution coefficient
f	volume fraction of dense phase
F	drag force, N
g	gravitational acceleration, m/s^2
g_0	radial distribution function
H	column height, m

H_d	heterogeneity index
N_{st}	mass-specific energy consumption for suspending and transporting particles, W/kg
N_T	total mass-specific energy, W/kg
p	pressure, Pa
Re	Reynolds number
u	actual or real velocity, m/s
U	superficial velocity, m/s
U_{mf}	superficial gas velocity at minimum fluidization, m/s
U_{slip}	superficial slip velocity, m/s
u_t	terminal velocity of a single particle, m/s

Greek letters

β	drag coefficient, kg/(m^{3}s)
γ_s	collisional energy dissipation, J/(m^{3}s)
Δt	time step, s
ε_g	voidage
ε_{gc}	voidage of dense phase
ε_{gf}	voidage of dilute phase
ε_{mf}	incipient/minimum fluidization voidage
ε_{sc}	solids concentration in the dense phase
ε_{sf}	solids concentration in the dilute phase
ε_{max}	maximum voidage for particle aggregation
$\varepsilon_{s,max}$	maximum close packing solids concentration
Θ_s	granular temperature, m^2/s^2
I	unit tensor
I_{2D}	second invariant of the deviatoric stress tensor
κ_s	diffusion coefficient for granular energy, Pa s
λ	bulk viscosity, Pa s
μ	viscosity, Pa s
ρ	density, kg/m^3
τ	stress tensor, Pa
φ	specularity coefficient
Φ	angle of internal friction (°)

Subscripts

b	bubble
c	dense phase
f	dilute phase
g	gas phase
gc	gas in dense-phase
gf	gas in dilute-phase
i	meso-scale interphase

	mf	minimum fluidization
	p	particle
	s	solid phase
	sc	dense-phase solid
	sf	dilute-phase solid

Appendix

Relevant parameters and definitions used in the development of this bubble-based EMMS mixture model are summarized in Table A.1.

Table A.1 Summary of parameters and definitions used in the current bubble-based EMMS mixture model

	Microscale Dense Phase		Interphase Voids	
	Fluid	Particles	Void	Suspension
Characteristic diameter	d_p		d_b	
Voidage	ε_{gc}		$1-f$	
Density	$\rho_{mc}=\varepsilon_{gc}\rho_g+(1-\varepsilon_{gc})\rho_p$		$\rho_{mi}=f\rho_{mc}+(1-f)\rho_g$	
Superficial Slip Velocity	$U_{slip,c}=U_{gc}-\dfrac{\varepsilon_{gc}}{1-\varepsilon_{gc}}U_{sc}$		$U_{slip,i}=f\left(U_{gf}-U_e\right)$	
Number Density	$m_c=\dfrac{(1-\varepsilon_{gc})}{\dfrac{\pi}{6}d_p^{\ 3}}$		$m_i=\dfrac{1-f}{\dfrac{\pi}{6}d_b^{\ 3}}$	
Characteristic Reynolds Number	$Re_c=\dfrac{d_p\rho_g U_{slip,c}}{\mu_g}$		$Re_i=\dfrac{d_b\rho_{mc}U_{slip,i}}{\mu_{mc}}$	
Drag coefficient for single entity	$C_{d0,c}=\dfrac{(24+3.6Re_c^{\ 0.687})}{Re_c}$		$C_{d0,i}=\begin{cases}38Re_i^{-1.5} & 0<Re_i\leq 1.8 \\ 2.7+\dfrac{24}{Re_i} & Re_i>1.8\end{cases}$	
Drag force each entity	$F_c=\dfrac{\rho_g}{2}\left(\dfrac{\pi}{4}d_p^{\ 2}\right)C_{d0,c}\varepsilon_{gc}^{\ -4.7}U_{slip,c}^{\ 2}$		$F_i=\dfrac{\rho_{mc}}{2}\left(\dfrac{\pi}{4}d_b^{\ 2}\right)C_{d0,i}\ f^{\ -0.5}U_{slip,i}^{\ 2}$	

15

Drag force in unit volume	$m_c F_c$	$m_l F_i$
Objective Function	$\left(N_{st,mix}\right)_b = \dfrac{1}{(1-\varepsilon_g)\rho_p}\left[\left(\dfrac{f(\rho_{mc}-\rho_{mi})}{(1-f)}\right)fU_{fc} + f_b U_f\right]g$	

The governing equations and constitutive closures of the two-fluid model are summarized in Table A.2.

Table A.2 Governing equations and constitutive closures for the two-fluid model

Continuity equation (k=g, s)	$\dfrac{\partial\left(\varepsilon_k\rho_k\right)}{\partial t} + \nabla\cdot\left(\varepsilon_k\rho_k\mathbf{u}_k\right) = 0$
Momentum equation (k= g, s; l = s, g)	$\left[\dfrac{\partial\varepsilon_k\rho_k\mathbf{u}_k}{\partial t} + \nabla\cdot(\varepsilon_k\rho_k\mathbf{u}_k\mathbf{u}_k)\right] = -\varepsilon_k\nabla p_g + \nabla\cdot\boldsymbol{\tau}_k + \varepsilon_g\rho_g\mathbf{g} + \beta\left(\mathbf{u}_l - \mathbf{u}_k\right)$
Gas phase stress	$\boldsymbol{\tau}_g = 2\mu_g\mathbf{S}_g + \varepsilon_g\lambda_g\nabla\cdot\mathbf{u}_g$
Particle phase stress tensor	$\boldsymbol{\tau}_s = [-p_s + \varepsilon_s\lambda_s\nabla\cdot\mathbf{u}_s]\mathbf{I} + 2\mu_s\mathbf{S}_s$
Deformation rate	$\mathbf{S}_k = \dfrac{1}{2}\varepsilon_k[\nabla\mathbf{u}_k + \left(\nabla\mathbf{u}_k\right)^T] - \dfrac{1}{3}\varepsilon_k\nabla\cdot\mathbf{u}_k\mathbf{I}$
Particle phase pressure	$p_s = \varepsilon_s\rho_p\Theta_s + 2(1+e)\varepsilon_s^2 g_0\rho_p\Theta_s$
Solid phase shear viscosity	$\mu_s = \mu_{s,col} + \mu_{s,kin} + \mu_{s,fr}$ $\mu_{s,col} = \dfrac{4}{5}\varepsilon_s^2\rho_p d_p g_0\left(1+e\right)\sqrt{\dfrac{\Theta_s}{\pi}}$ $\mu_{s,kin} = \dfrac{10\rho_p d_p\sqrt{\Theta_s\pi}}{96\varepsilon_s\left(1+e\right)g_0}\left[1 + \dfrac{4}{5}g_0\varepsilon_s\left(1+e\right)\right]^2$ $\mu_{s,fr} = \dfrac{\rho_p\sin\phi}{2\sqrt{\mathbf{I}_{2D}}}$
Bulk viscosity	$\lambda_g = 0, \quad \lambda_s = \dfrac{4}{3}\varepsilon_s^2\rho_p d_p g_0\left(1+e\right)\left(\dfrac{\Theta_s}{\pi}\right)^{1/2}$

Radial distribution function	$$g_0 = \left[1 - \left(\varepsilon_s \middle/ \varepsilon_{s,max} \right)^{\!1/3} \right]^{-1}$$
Granular temperature equation	$$\frac{3}{2} \left[\frac{\partial}{\partial t} \left(\varepsilon_s \rho_p \Theta_s \right) + \nabla \cdot \left(\varepsilon_s \rho_p \mathbf{u_s} \Theta_s \right) \right] = \boldsymbol{\tau}_s : \left(\nabla \cdot \mathbf{u_s} \right) + \nabla \cdot \mathbf{q} - \gamma - 3\beta\Theta_s$$
Collisional energy dissipation	$$\gamma_s = \left(1 - e^2 \right) \varepsilon_s^2 \rho_p g_0 \frac{12}{d_p \sqrt{\pi}} \Theta_s^{3/2}$$
Flux of fluctuating energy	$$\mathbf{q} = -\kappa_s \nabla \Theta_s$$
Conductivity of fluctuating energy	$$\kappa_s = \frac{2\kappa^k \left[1 + \frac{6}{5}(1+e)\varepsilon_s g_0 \right]^2}{(1+e)g_0} + \kappa^c$$ $$\kappa^k = \frac{75}{384} d_p \rho_p \sqrt{\Theta_s \pi}$$ $$\kappa^c = 2\varepsilon_s^2 \rho_p d_p g_0 (1+e) \sqrt{\frac{\Theta_s}{\pi}}$$
Drag coefficient for Gidaspow drag model	$$\begin{cases} \varepsilon_g > 0.8 \quad \beta_{WY} = \frac{3}{4} \frac{\varepsilon_g(1-\varepsilon_g)}{d_p} \rho_g C_{D0} \left| \mathbf{u_g} \text{-} \mathbf{u_s} \right| \varepsilon_g^{-2.7} \\[2mm] \varepsilon_g \le 0.8 \quad \beta_{Ergun} = 150 \frac{\mu_g (1-\varepsilon_g)^2}{\varepsilon_g d_p^2} + 1.75 \frac{\rho_g (1-\varepsilon_g) \left| \mathbf{u_g} \text{-} \mathbf{u_s} \right|}{d_p} \end{cases}$$ $$\begin{cases} Re_p < 1000 \quad C_{D0} = \frac{24 + 3.6\,Re_p^{0.687}}{Re_p} \\[2mm] Re_p \ge 1000 \quad C_{D0} = 0.44 \end{cases}$$ $$Re_p = \frac{\rho_g \varepsilon_g d_p \left| u_g \text{-} u_s \right|}{\mu_g}$$
Drag coefficient for EMMS drag model	$$\beta = \beta_{WY} H_D = \frac{3}{4} \frac{\varepsilon_g(1-\varepsilon_g)}{d_p} \rho_g C_{D0} \left| \mathbf{u_g} \text{-} \mathbf{u_s} \right| \varepsilon_g^{-2.7} H_d$$ H_d for Group-A particles

$$\begin{cases} \varepsilon_{mf} \le \varepsilon_g \le 0.518 & \dfrac{1}{\left(1052.744 - 5315.6\varepsilon_g - 6715.74\varepsilon_g^{\,2} - 0.0386\right)} \\[3mm] 0.518 < \varepsilon_g \le 0.749 & 0.52253 - 2.09986\varepsilon_g + 2.79274\varepsilon_g^{\,2} - 0.95728\varepsilon_g^{\,3} \\[3mm] \varepsilon_g > 0.749 & 0.55584\varepsilon_g^{\,5.512} \end{cases}$$

H_d for Group-B particles

$$\begin{cases} 0.425 \le \varepsilon_g \le 0.878 & 6.40656 - 24.30788\varepsilon_g + 33.91204\varepsilon_g^{\,2} - 15.65392\varepsilon_g^{\,3} \\[3mm] 0.878 < \varepsilon_g \le 0.961 & (4.3584 \times 10^{-4})(1 + \varepsilon_g)^{11.498} \\[3mm] \text{Else} & 1.0 \end{cases}$$

List of Tables

List of Figures

Figure 1 Heterogeneity index H_d as a function of mean voidage for the turbulent fluidized systems used for simulation.

Figure 2 Schematic of the turbulent fluidized bed setup used for simulation.

Figure 3 (a) Time-averaged profiles of voidage along the bed height for different grid sizes; (b) Instantaneous solid fraction in the bed.

Figure 4 Comparison of results for EMMS drag model with Gidaspow drag model: (a) Time-averaged axial voidage profile; (b) Time-averaged radial solid fraction profiles at a height of 0.198m; (c) Time-averaged radial solid fraction profiles at a height of 0.138m.

Figure 5 Effect of wall boundary condition on the time-averaged profiles for both EMMS and Gidaspow drag model: (a) Axial voidage profiles; (b) Radial solid fraction profiles at a height of 0.198m; (c) Radial solid fraction profiles at a height of 0.138m.

Figure 6 Simulation results of turbulent fluidized bed with Group-A particles using EMMS drag model: (a) Snapshot of instantaneous solid fraction in the bed; (b) Axial voidage profile; (c) Time averaged snapshot of solid fraction in the bed.

References

[1] G.L. Matheson, W.A. Herbst, P.H. Holt, Characteristics of Fluid-Solid Systems, Industrial & Engineering Chemistry, 41 (1949) 1098-1104.

[2] H.T. Bi, N. Ellis, I.A. Abba, J.R. Grace, A state-of-the-art review of gas–solid turbulent fluidization, Chemical Engineering Science, 55 (2000) 4789-4825.

[3] J. Li, M. Kwauk, Particle-fluid two-phase flow: the energy-minimization multi-scale method, Metallurgy Industry Press, Beijing1994.

[4] M. Rhodes, What is turbulent fluidization?, Powder Technology, 88 (1996) 3-14.

[5] J.R. Grace, Reflections on turbulent fluidization and dense suspension upflow, Powder Technology, 113 (2000) 242-248.

[6] R.H. Venderbosch, The role of clusters in gas-solids reactors. An experimental study., Department of Chemical Engineering, University of Twente, Enschede, Netherlands, 1998, pp. 208.

[7] F. Berruti, T.S. Pugsley, L. Godfroy, J. Chaouki, G.S. Patience, Hydrodynamics of circulating fluidized bed risers: A review, The Canadian Journal of Chemical Engineering, 73 (1995) 579-602.

[8] A. Gungor, N. Eskin, Hydrodynamic modeling of a circulating fluidized bed, Powder Technology, 172 (2007) 1-13.

[9] D. Gidaspow, Multiphase Flow and Fluidization: Continuum and Kinetic Theory Descriptions, 1st ed., Academic Press, San Diego1994.

[10] V. Jiradilok, D. Gidaspow, S. Damronglerd, W.J. Koves, R. Mostofi, Kinetic theory based CFD simulation of turbulent fluidization of FCC particles in a riser, Chemical Engineering Science, 61 (2006) 5544-5559.

[11] J. Gao, X. Lan, Y. Fan, J. Chang, G. Wang, C. Lu, C. Xu, CFD modeling and validation of the turbulent fluidized bed of FCC particles, AIChE Journal, 55 (2009) 1680-1694.

[12] J. Chang, G. Wang, X. Lan, J. Gao, K. Zhang, Computational Investigation of a Turbulent Fluidized-bed FCC Regenerator, Industrial & Engineering Chemistry Research, 52 (2013) 4000-4010.

[13] X. Gao, C. Wu, Y.-w. Cheng, L.-j. Wang, X. Li, Experimental and numerical investigation of solid behavior in a gas–solid turbulent fluidized bed, Powder Technology, 228 (2012) 1-13.

[14] B. Lu, W. Wang, J. Li, Searching for a mesh-independent sub-grid model for CFD simulation of gas-solid riser flows, Chemical Engineering Science, 64 (2009) 3437-3447.

[15] S. Sundaresan, Modeling the hydrodynamics of multiphase flow reactors: Current status and challenges, AIChE Journal, 46 (2000) 1102-1105.

[16] K. Agrawal, P.N. Loezos, M. Syamlal, S. Sundaresan, The role of meso-scale structures in rapid gas-solid flows, Journal of Fluid Mechanics, 445 (2001) 151-185.

[17] Y. Igci, A.T. Andrews, S. Sundaresan, S. Pannala, T. O'Brien, Filtered two-fluid models for fluidized gas-particle suspensions, AIChE Journal, 54 (2008) 1431-1448.

[18] K. Hong, W. Wang, Q. Zhou, J. Wang, J. Li, An EMMS-based multi-fluid model (EFM) for heterogeneous gas–solid riser flows: Part I. Formulation of structure-dependent conservation equations, Chemical Engineering Science, 75 (2012) 376-389.

[19] S. Benyahia, S. Sundaresan, Do we need sub-grid scale corrections for both continuum and discrete gas-particle flow models?, Powder Technology, 220 (2012) 2-6.

[20] M. Syamlal, S. Pannala, Multiphase Continuum Formulation for Gas-Solids Reacting Flows, in: S. Pannala, M. Syamlal, T.J. O'Brien (Eds.) Computational Gas-Solids Flows and Reacting Systems: Theory, Methods and Practice, IGI Global2010, pp. 2-61.

[21] D.Z. Zhang, W.B. VanderHeyden, The effects of mesoscale structures on the macroscopic

momentum equations for two-phase flows, International Journal of Multiphase Flow, 28 (2002) 805-822.

[22] L. Huilin, S. Qiaoqun, H. Yurong, S. Yongli, J. Ding, L. Xiang, Numerical study of particle cluster flow in risers with cluster-based approach, Chemical Engineering Science, 60 (2005) 6757-6767.

[23] G.J. Heynderickx, A.K. Das, J. De Wilde, G.B. Marin, Effect of Clustering on Gas−Solid Drag in Dilute Two-Phase Flow, Industrial & Engineering Chemistry Research, 43 (2004) 4635-4646.

[24] N. Yang, W. Wang, W. Ge, J. Li, CFD simulation of concurrent-up gas-solid flow in circulating fluidized beds with structure-dependent drag coefficient, Chemical Engineering Journal, 96 (2003) 71-80.

[25] W. Wang, J. Li, Simulation of gas - solid two-phase flow by a multi-scale CFD approach - Extension of the EMMS model to the sub-grid level, Chemical Engineering Science, 62 (2007) 208 - 231.

[26] J. Wang, W. Ge, J. Li, Eulerian simulation of heterogeneous gas–solid flows in CFB risers: EMMS-based sub-grid scale model with a revised cluster description, Chemical Engineering Science, 63 (2008) 1553-1571.

[27] Z. Shi, W. Wang, J. Li, A bubble-based EMMS model for gas–solid bubbling fluidization, Chemical Engineering Science, 66 (2011) 5541-5555.

[28] K. Hong, Z. Shi, A. Ullah, W. Wang, Extending the bubble-based EMMS model to CFB riser simulations, Powder Technology, 266 (2014) 424-432.

[29] P. Li, X. Lan, C. Xu, G. Wang, C. Lu, J. Gao, Drag models for simulating gas–solid flow in the turbulent fluidization of FCC particles, Particuology, 7 (2009) 269-277.

[30] K. Hong, Z. Shi, W. Wang, J. Li, A structure-dependent multi-fluid model (SFM) for heterogeneous gas–solid flow, Chemical Engineering Science, 99 (2013) 191-202.

[31] M. Manninen, V. Taivassalo, S. Kallio, On the mixture model for multiphase flow, 1996.

[32] M. Horio, A. Nonaka, A generalized bubble diameter correlation for gas-solid fluidized beds, AIChE Journal, 33 (1987) 1865-1872.

[33] C. Wen, Y. Yu, Mechanics of fluidization, Chem. Eng. Prog. Symp. Ser., 1966, pp. 100-111.

[34] A. Ullah, W. Wang, J. Li, An EMMS based mixture model for turbulent fluidization, 11th International Conference on Fluidized Bed TechnologyBeijing, China, 2014, pp. 267-272.

[35] B.G.M. van Wachem, J.C. Schouten, C.M. van den Bleek, R. Krishna, J.L. Sinclair, Comparative analysis of CFD models of dense gas–solid systems, AIChE Journal, 47 (2001) 1035-1051.

[36] F. Song, W. Wang, K. Hong, J. Li, Unification of EMMS and TFM: structure-dependent analysis of mass, momentum and energy conservation, Chemical Engineering Science, 120 (2014) 112-116.

[37] S. Benyahia, Analysis of model parameters affecting the pressure profile in a circulating fluidized bed, AIChE Journal, 58 (2012) 427-439.